Perception of forbidden colors in retinally stabilized equiluminant images: an indication of softwired cortical color opponency?

Vincent A. Billock

Logicon, Inc., U.S. Air Force Research Laboratory, P.O. Box 317258, Dayton, Ohio 45437-7258

Gerald A. Gleason and Brian H. Tsou

U.S. Air Force Research Laboratory, Wright Patterson Air Force Base, Ohio 45433

Received August 28, 2000; revised manuscript received April 13, 2001; accepted April 13, 2001

In color theory and perceptual practice, two color naming combinations are forbidden—reddish greens and bluish yellows—however, when multicolored images are stabilized on the retina, their borders fade and filling-in mechanisms can create forbidden colors. The sole report of such events found that only some observers saw forbidden colors, while others saw illusory multicolored patterns. We found that when colors were equiluminant, subjects saw reddish greens, bluish yellows, or a multistable spatial color exchange (an entirely novel perceptual phenomena); when the colors were nonequiluminant, subjects saw spurious pattern formation. To make sense of color opponency violations, we created a soft-wired model of cortical color opponency (based on winner-take-all competition) whose opponency can be disabled. © 2001 Optical Society of America

OCIS codes: 330.1690, 330.1720, 330.4060.

1. INTRODUCTION

Perhaps the most surprising result in the perceptual literature is Crane and Piantanida's report that reddish green and yellowish blue colors can be created—in violation of Hering's laws of color opponency—by stabilizing bipartite colored fields and allowing the colors to bleed across the perceptually fading border.[1] They found that some observers see novel mixture colors undreamt of in Hering's philosophy, while other observers perceive unstable islands of one color floating in a sea of the other, or ultrafine colored textures. These results—controversial in their time and never replicated—largely predated highly relevant work on the effects of equiluminance on perception of unstabilized images[2] and on the possibility of nonlocal color opponency in visual cortex.[3–7] This kind of soft-wired opponency may be disruptable.

2. EXPERIMENTS

First we investigated why some of Crane and Piantanida's subjects saw mixture colors while others saw spurious pattern formation.[1] Crane and Piantanida's subjects presumably vary in spectral sensitivity, just as the general population does; their stimuli would have more luminance contrast for some observers than for others, and this might affect how completely the border between the two sides fades. Image fragmentation is reported by some observers for stabilized images,[8] and unstable border form/contrast occurs for some equiluminant images.[9] If either condition were capable of destabilizing or degrading stimulus-driven segmentation, then perhaps segmentation would fail completely for equiluminous stabilized borders. There is precedent for expecting such a synergy: Luminance-minimized borders fade more rapidly and completely when steadily fixated[9]; elevation of detection thresholds for stabilized equiluminant gratings is much larger than for stabilized nonequiluminant gratings.[10] To study this possibility we used a dual Purkinje image eye tracker to retinally stabilize bipartite color fields whose hues and achromatic border contrast were controlled.[11] We found that texture formation suggestive of self-organized pattern formation or spurious segmentation occurred only if there was a strong luminance difference between the two colors; if the colors were made equiluminant, no segmentation occurred and mixture colors were obtained from the filling-in process. If equiluminous red/green or blue/yellow bipartite fields were used, then subjects reported reddish greens or bluish yellows, in violation of Hering's laws. The quality of the experience varied between observers and over time. Some subjects (4 out of 7) described transparency phenomena[12]—as though the opponent colors originated in two depth planes and could be seen, one through the other. Other times, the border would disappear and the subjects (5 out of 7) reported a gradient of color that ran from, say, red on the left to green on the right with a large region in between that seemed both red and green.[13] Our subjects (like those in Ref. 1) were tongue-tied in their descriptions of these colors, using terms like "green with a red sheen," or "red with green highlights." Typically the perception of these phenomena would last a few seconds before the entire field would switch abruptly to

blackness or nothingness.[14] Then the red/green bipartite field would regenerate, either spontaneously, or in response to a blink. On occasion (4 out of 7 subjects) the percept was a homogeneous mixture color whose red and green components were as clear and as compelling as the red and blue components of a purple. This percept tended to last longer than the gradient phenomenon. Experience may be a factor in what is seen; many subjects did not report non-Hering mixtures until after several trials, and in general, transparency and gradient effects preceded perception of homogeneous mixture colors. This bears on arguments that novel color percepts may be precluded by lack of early experience during perceptual development.[15,16] Clearly the strongest form of this argument is not supported, but the effects of experience suggest that a gradual sensory reorganization may be taking place. Interestingly, after our experiments, two subjects noted independently that reddish-green and yellowish-blue colors could now be imagined. We also discovered an entirely novel percept (4 out of 7 subjects) in which the red and green (or blue and yellow) bipartite fields abruptly exchange sides before fading or returning to the veridical percept; a digital-like switching phenomenon that may indicate a nonlinear dynamic process in operation. Switching, unlike non-Hering colors, occurred for both equiluminous and nonequiluminous stimuli. One subject—an expert psychophysical observer—saw a 90° reorganization of the bipartite field so that red and green were now over and under rather than side by side, which precludes a simple explanation based on the observer's reporting a negative afterimage while the perception of the actual stimulus is somehow masked (i.e., the Bidwell effect).

We also experimented with making the bipartite fields strongly nonequiluminant (e.g., green 2–5 times more radiant than green flicker-matched to red). Under such conditions, subjects seldom saw non-Hering mixture colors but instead reported spatially structured phenomena. Again description was difficult, but subjects typically saw a portion of the border fade and be replaced with speckled patterns of red and green, whose structure was hard to pin down. Sometimes the perception was like "red dust on a field of green." Often one had the impression of a texture like those seen at the resolution/contrast limit. A diffusion-like spreading was often seen. Sometimes a foveal-like region at the center of the field, encapsulating a piece of border, would remain intact while color mixtures all about it were in flux. Occasionally a transparent film of one color would creep over the other near their border. At times one color would eclipse the other.

3. MODELING

At first glance our results (and those of Crane and Piantanida) are hard to reconcile in a simple color-opponent framework. Perception of reddish green and bluish yellow are thought to be precluded by the existence of color-opponent mechanisms that difference signals from long-, medium-, and short-wavelength-sensitive (L, M, and S, respectively) receptors. Such mechanisms are found from retina to cortex and come in two varieties: red–green (r–g) and blue–yellow (b–y). The response of the r–g system is either reddish, greenish, or inactive (for unique yellow and blue) and similarly for the b–y system. Crane and Piantanida suggest that opponency violations may be achieved by a nonopponent filling-in mechanism,[1] distal to the opponent stages. However, there may be no need for an extra stage of processing. Recent models of cortical color processing suggest that cortical color opponency may not be based on hard-wired wavelength opponency within a single cell but rather on (potentially fragile) interactions between cortical color-sensitive cells.[3,5] Here we present a simple model that consists of a winner-take-all network of color-labeled wavelength-selective cortical cells. We show that with an appropriate choice of parameters and a simple assumption about how stabilization affects some of these parameters, the model can account for both classic hue cancellation measurements and our qualitative observations of color-opponency violations. Thus the model provides a framework in which to understand the new observations without abandoning the empirical observations that underlie many current models of opponency. For simplicity and brevity we present only the model for the red–green opponent system.

As in all modern models of color vision, we assume that the first stage of visual processing is transduction of light by three classes of cone photoreceptors with spectral sensitivities [shown in Fig. (1a)]. Signals from the cones are assumed to be combined in an opponent fashion to produce opponent signals in retinal ganglion cells [Fig. (1b)]. This opponency is lost when the retinal ganglion cell signals are passed to some cortical cells that filter and rectify[17] the afferent signal, resulting in the spectral sensitivities shown in Fig. (1c) and modeled by Eqs. (1)–(3):

$$\mathrm{LC}^* = \mathrm{Rect}[\mathrm{LC}] = \mathrm{Rect}[(1 - kP_L)L - kP_M M], \tag{1}$$

$$\mathrm{MC}^* = \mathrm{Rect}[\mathrm{MC}] = \mathrm{Rect}[(1 - kP_\mathrm{M})\mathrm{M} - kP_\mathrm{L}\mathrm{L}], \tag{2}$$

$$\mathrm{SC}^* = \mathrm{Rect}[\mathrm{SC}] = \mathrm{Rect}[(1 - kP_\mathrm{S})\mathrm{S} - k(P_\mathrm{M}\mathrm{M} + P_\mathrm{L}\mathrm{L})] \tag{3}$$

where LC, MC, and SC represent average members of the L-cone center, M-cone center, and S-cone center cell populations, respectively, Rect[x] is a cortical rectifier that reflects the lack of a maintained discharge, k is the center/surround integrated strength ratio, and P_L, P_M, and P_S (the proportions of L, M, and S cones on the retina) sum to 1.[18] (For generality, we assume mixed cone surrounds of variable strength with respect to the center.)[3,18,19] Cortical cells with relatively narrow spectral responses such as LC*, MC*, and SC* have been studied previously.[20–22] A fragile opponency can be implemented by allowing wavelength-selective cells to feed into a winner-take-all competition network. For example, the simplest possible implementation of a red–green competitive-opponent channel seems to be

$$\mathrm{d}\omega_R/\mathrm{d}t = \omega_R[\mathrm{LC}^*(\lambda) - (a\omega_R + b\omega_G + c\omega_V)], \tag{4}$$

$$\mathrm{d}\omega_G/\mathrm{d}t = \omega_G[\mathrm{MC}^*(\lambda) - (d\omega_G + e\omega_R + f\omega_V)], \tag{5}$$

$$\mathrm{d}\omega_V/\mathrm{d}t = \omega_V[\mathrm{SC}^*(\lambda) - (h\omega_V + i\omega_R + j\omega_G)]. \tag{6}$$

Where R, G, and V are competing cortical cell classes whose wavelength-dependent activity (ω_R, ω_G, ω_V) are labeled for long-wavelength redness, greenness, and

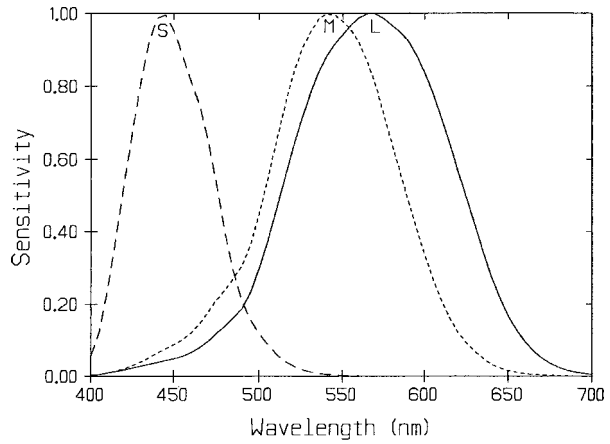

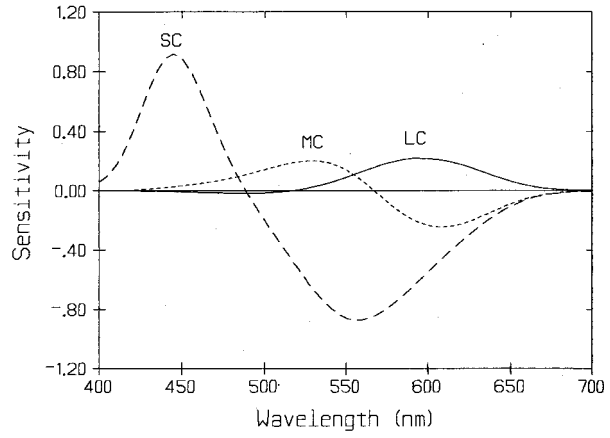

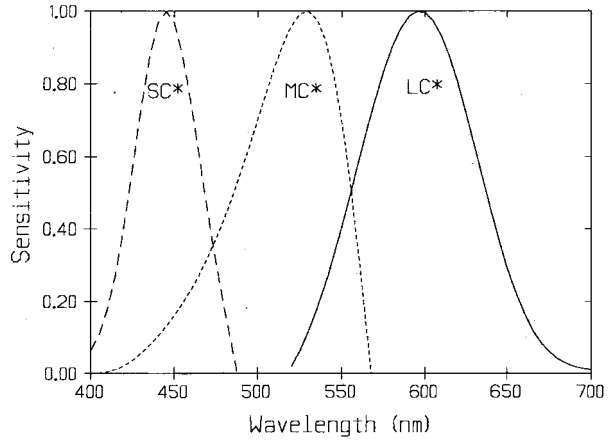

Fig. 1. Early mechanisms in multistage color processing. (a) L-, M- and S-cone spectral sensitivities.[27] (b) Chromatic sensitivities of retino-geniculate mechanisms from Eqs. (1)–(3), with receptive field centers driven by L, M, and S cones and surrounds driven by a mixture of cones (a plausible, but not crucial, assumption). Computed from the unrectified portions of Eqs. (1)–(3) with $k = 0.95$, $P_L = 0.625$, $P_M = 0.3125$, $P_S = 0.0625$. (c) Cortical wavelength-selective mechanisms produced by filtering and rectifying the outputs of units like those of Fig. 1(b). Normalized for comparison with Fig. 1(a).

short-wavelength redness, respectively.[23] We make no claims for the physiological implementation of this set of equations, but note that similar winner-take-all networks have proven useful in modeling other aspects of visual perception.[24] Often these nonlinear dynamic models are used to address the detailed dynamics of the system (e.g., multistability and hysteresis), but here the quantitative aspects of the model are intended to show that this unfamiliar form of opponency can reproduce the quantitative details of color opponency found psychophysically. Figure 2 shows the good fit of this model to Jameson and Hurvich's seminal data.[25–27] However, the findings on color opponency that we want to understand are qualitative, so it is worthwhile to understand Eqs. (4)–(6) on a qualitative basis. The equations describe the growth and decay of neural firing rates in each labeled line. The coefficients capture the possible interactions of the labeled

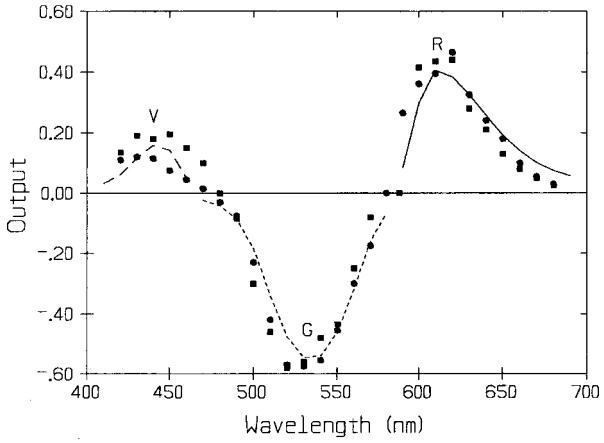

Fig. 2. A winner-take-all competition model of classic red–green color opponency. Nonlinear dynamic interactions between units driven by the mechanisms in Fig. 1(c) give rise to Hering-like color opponency. Points are Jameson and Hurvich's[25] two-observer measurements of the red–green color-opponent response. The plotted line is the least-squares fit (to the average of the observers) of competitive mechanisms labeled for hue [Eqs. (4)–(6)], with each lobe being the output of one equation (integrated numerically[25]) and graphed with conventional polarity (which is arbitrary). Under some conditions this kind of opponency can be deactivated, permitting violations of color opponency.

Table 1. Parameters Used for Calculation in Fig. 2[a]

Parameter	Value	Description
K	0.95	Center/surround strength ratio for P cells
P_L	0.6250	Fraction of L cones
P_M	0.3125	Fraction of M cones
P_S	0.0625	Fraction of S cones
a	0.49027	Self-inhibition of activity (ω_R) in red labeled system
d	0.35462	Self-inhibition of activity (ω_G) in green labeled system
h	5.9987	Self-inhibition of activity (ω_V) in red labeled system
b^*	0.07537	Coupling of ω_G to ω_R
c^*	−0.29789	Coupling of ω_V to ω_R
e^*	7.7816	Coupling of ω_R to ω_G
f^*	−0.72997	Coupling of ω_V to ω_G
i^*	−594.77	Coupling of ω_R to ω_V
j^*	67.621	Coupling of ω_G to ω_V

[a] Parameters marked "*" are set to zero for the calculation in Fig. 3.

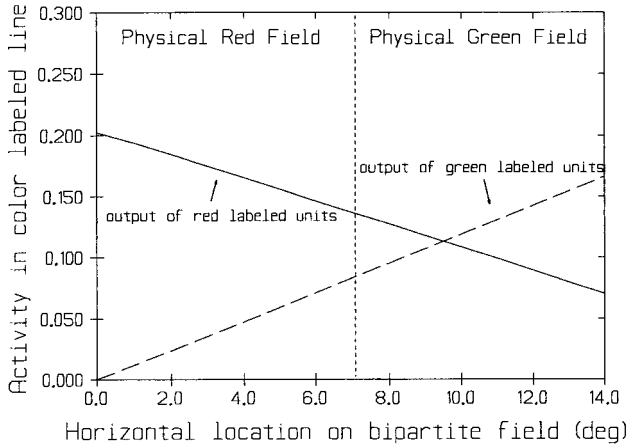

Fig. 3. If competition between units in the winner-take-all network is blocked, then red- and green-labeled units are free to signal red and green on each side of the bipartite field. This figure shows red- and green-labeled activity gradients [Eqs. (9) and (10)] that result from diffusion-like filling-in processes occurring from each side of a red/green bipartite field of 14 deg horizontal extent.

lines. If each color-labeled mechanism were neurally isolated from the others (e.g., if $b, c, e, f, i, j = 0$), then each mechanism's activity grows logistically to a saturation value (at equilibrium: $\omega_R = \mathrm{LC}^*/a$; $\omega_G = \mathrm{MC}^*/d$; $\omega_V = \mathrm{SC}^*/h$). If two or more mechanisms are active and their interaction terms are nonzero, they interfere with each other's growth rates; in practice, at any given wavelength, one mechanism wins this competition and drives the other mechanisms into inactivity, which is an opponent process. If the competitive interactions can be disabled (see below), then such a system can signal reddish green on one side of a field and greenish red on the other. By itself, however, this could not explain smooth gradients or uniform color mixtures like those experienced by most of our observers. These results are more consistent with a diffusive-like color mixing that could be modeled by adding diffusion terms to Eqs. (4)–(6).[28–31] For our red/green stimulus, which has dominant wavelengths of approximately 610 and 545 nm, respectively, (inducing no ω_V activity), and which varies only in the horizontal direction, a reduced system suffices.

$$\partial\omega_R/\partial t = \omega_R[\mathrm{LC}^*(\lambda) - a\,\omega_R - b\,\omega_G] + D_R\partial^2\omega_R/\partial x^2, \tag{7}$$

$$\partial\omega_G/\partial t = \omega_G[\mathrm{MC}^*(\lambda) - d\,\omega_G - e\,\omega_R] + D_G\partial^2\omega_G/\partial x^2, \tag{8}$$

where D_R and D_G are diffusion rate constants. These Lotka–Volterra diffusion equations can produce color gradients like the ones that our subjects experienced. Let b and e be set to zero (the nonopponent condition). At the outside (unstabilized) edge ($x = 0$ deg) of the red field, the red-labeled activity is clamped to a value of $\omega_R = \mathrm{LC}^*(610\,\mathrm{nm})/a$. At the outside of the green edge ($x = 14$ deg), the red-labeled activity is clamped at $\mathrm{LC}^*(545)/a$. Similar behavior holds for the green-labeled line, except that MC* has no sensitivity to 610-nm lights. At steady state the activity in the labeled lines forms ramp-like gradients in the interior (stabilized) area[30]:

$$\omega_R(x) = \mathrm{LC}^*(610)/a - x[\mathrm{LC}^*(610) - \mathrm{LC}^*(545)]/14a. \tag{9}$$

$$\omega_G(x) = \mathrm{MC}^*(545)/d - (14 - x)[\mathrm{MC}^*(545)]/14d. \tag{10}$$

Figure 3 illustrates the resulting gradients. Such reaction–diffusion systems are also capable of creating spatial patterns (self-organized pattern formation) by their interactions (if the competition terms are not disabled).[28,32] Perceptually such a result would manifest as an illusory texture, such as those sometimes seen in these experiments when luminance cues are present.

4. DISCUSSION

The physiological mechanisms by which competition interactions could be disabled are unknown.[33–35] However, it is clear from our experiments that there is a synergistic effect of equilumininance and stabilization on both the salience of the border and the failure of color opponency. This border synergy may be related to cross-modal construction, a tendency that some connectionist network models of segmentation show for improved performance when two or more visual modalities signal common borders.[36] What our model of color opponency and these segmentation models have in common is the distributed nature of the processing. It may be possible to study the synergy of equiluminance and stabilization on both segmentation and color perception by using multifocal recording techniques developed for studying distributed processing,[37] or functional imaging (although integrating image-stabilization technology in a functional imaging system may be technically challenging). Other venues for continued work would be to study and model the dynamics of perceptual alternations during stabilization or the spatial patterns seen in nonequiluminant stabilized images.

ACKNOWLEDGMENTS

We thank Eric Heft and Robert Schwartz for technical assistance; Carl Ingling, Allen Nagy, Scott Grigsby, Paul Havig, and Julie Beegan for serving as subjects; Dale Purves and Oliver Sacks for reviewing the manuscript; and Jeff Hovis for helpful suggestions.

Vincent A. Billock's e-mail address is vince.billock@wpafb.af.mil.

REFERENCES AND NOTES

1. H. D. Crane and T. P. Piantanida, "On seeing reddish green and yellowish blue," Science **221**, 1078–1080 (1983).
2. For a review see P. Cavanagh, "Vision at equiluminance," in *Limits of Vision*, Vol. 5 of Vision and Visual Dysfunction, J. J. Kulikowski, V. Walsh, and I. J. Murray, eds. (CRC Press, Boca Raton, Fla., 1991), pp. 234–250.
3. R. L. De Valois and K. K. De Valois, "A multistage vision model," Vision Res. **33**, 1053–1065 (1993).
4. N. C. Cottaris and R. L. De Valois, "Temporal dynamics of chromatic tuning in macaque primary visual cortex," Nature **395**, 896–900 (1998).
5. V. A. Billock, "A chaos theory approach to some intractable problems in color vision," Invest. Ophthalmol. Visual Sci. **38**, 254 (1997).

6. V. A. Billock, A. J. Vingrys, and P. E. King-Smith, "Opponent color detection threshold asymmetries may result from reduction of ganglion cell subpopulations," Visual Neurosci. **11**, 99–109 (1994).
7. R. L. De Valois, K. K. De Valois, E. Switkes, and L. Mahon, "Hue scaling of isoluminant and cone specific lights," Vision Res. **37**, 885–897 (1997).
8. Stabilized images often fragment upon stabilization; the fragments fade and revive in groupings that obey Gestalt-like laws. R. M. Prichard, W. Heron, and D. O. Hebb, "Visual perception approached by the method of stabilized images," Can. J. Psychol. **14**, 67–77 (1960).
9. S. L. Buck, F. Frome, and R. M. Boynton, "Initial distinctness and subsequent fading of minimally distinct borders," J. Opt. Soc. Am. **67**, 1126–1128 (1977).
10. D. H. Kelly, "Disappearance of stabilized chromatic gratings," Science **214**, 1257–1258 (1981).
11. We used a Generation 5 dual Purkinje image eye tracker (Fourward Technologies, El Cajon, Calif.), which transduces moving infrared reflections from cornea and lens. This signal is fed back to a servo-driven mirror to stabilize the image of a stimulus reflected therein (see Ref. 1). The primary subjects were two of the authors, but five additional observers, including outside color researchers, also participated. Because Ref. 1 reported difficulty characterizing non-Hering colors, we used only extremely experienced observers (all but one—a doctoral candidate in color vision—are professional psychophysicists). All subjects had normal color vision (gauged by anomaloscope and F_2 tritan test plates). Experiments were in accord with U.S. Air Force human-use protocols. Subjects were fixed by forehead and chin rests, with their left eyes patched and their right pupils dilated by 1 drop of 1% Tropicamide to facilitate tracking of the 4th Purkinje image. Red/green and blue/yellow bipartite fields were presented on a photometrically and colorimetrically calibrated VisionWorks (VRG, Inc., Durham, NH) display system. The two sides of the field could be equated for luminance by flicker photometry. The standard red field had CIE chromaticity coordinates of (0.631, 0.338) and a CIE luminance of 13.8 cd/m^2. The green field flicker matched to it had coordinates (0.287, 0.604). The blue field was (0.151, 0.061) and had a luminance of 8 cd/m^2 (the maximum available). The yellow field flicker matched to it consisted of equal mixtures of the red and green guns. Its CIE coordinates were (0.393, 0.525), which is considered a greenish-yellow location in CIE space but which appeared golden under experimental conditions. Refractive error and monitor distance were optically compensated. To achieve stabilization, subjects controlled mirror deflection circuit gain. Stabilization was checked by observations of eye movement effects on the position of colored borders relative to the unstabilized aperture. As in Ref. 1, the stabilized bipartite fields were viewed through unstabilized vertical occluders to reduce the incidence of image fading (which is otherwise severe). The visible stimulus subtended 14° horizontal×24° vertical.
12. The transparency effects are reminiscent of superimposition effects sometimes seen in binocular color mixtures (two subjects report luster effects similar to binocular luster). J. Hovis, "Review of dichoptic color mixing," Optom. Vision Sci. **66**, 181–190 (1989).
13. The gradient effect is seen for steadily fixated color pairs whose border stimulates only S cones. B. W. Tansley and R. M. Boynton, "A line, not a space, represents visual distinctness of borders formed by different colors," J. Opt. Soc. Am. **71**, 145–150 (1981). However, we found that gradients can be produced from any pair of equiluminous colors if stabilized.
14. Although image stabilization often induces gradual fading, most of our subjects (6 out of 7) reported simultaneously binocular abrupt transitions to pitch blackness or to complete loss of any visual sense; one psychophysicist characterized it as like the optic nerve being cut; another compared it with the visual blackout that accompanies manual carotid strangulation in the martial arts. This strikingly unnatural phenomenon is believed to be mediated by central mechanisms. R. W. Ditchburn, *Eye-Movements and Visual Perception* (Clarendon, Oxford, UK, 1973).
15. D. Hume, *Treatise on Human Nature* (Oxford U. Press, Oxford, UK, 1739/1955).
16. O. W. Sacks, *An Anthropologist on Mars: Seven Paradoxical Tales* (Vintage, New York, 1995).
17. One rationale for low-pass filtering (pooling) and rectification can be found in demultiplexing theory: V. A. Billock, "Cortical simple cells can extract achromatic information from the multiplexed chromatic and achromatic signals in the parvocellular pathway," Vision Res. **35**, 2359–2369 (1995). Other evidence is found in psychophysical data of subjects with low ganglion cell densities (Ref. 6). See Ref. 3 for a different but related approach.
18. V. A. Billock, "Consequences of retinal color coding for cortical color decoding," Science **274**, 2118–2119 (1996).
19. P. E. Lennie, P. W. Haake, and D. R. Williams, "The design of chromatically opponent receptive fields," in *Computational Models of Visual Processing*, M. S. Landy and J. A. Movshon, eds. (MIT Press, Cambridge, Mass., 1991), pp. 71–82.
20. S. Zeki, "Color coding in the cerebral cortex," Neuroscience (N.Y.) **9**, 741–756 (1983).
21. H. Komatsu, Y. Ideura, S. Kaji, and Y. Shigeru, "Color selectivity of neurons in the inferior temporal cortex of awake macaque monkey," J. Neurosci. **12**, 408–424 (1992).
22. P. Kaloudis, H. Friedman, C. Vemuri, and R. von der Heydt, "Color selectivity of metacontrast masking," Invest. Ophthalmol. Visual Sci. **39**, 407 (1998).
23. This is a highly modified version of the Lotka–Volterra population dynamics model; for review see S. Grossberg, "Nonlinear neural networks," Neural Networks **1**, 17–61 (1988).
24. H. R. Wilson, *Spikes, Decisions, and Actions: The Dynamical Foundations of Neuroscience* (Oxford U. Press, Oxford, UK, 1999).
25. Data of D. Jameson and L. M. Hurvich, "Some quantitative aspects of an opponent-colors theory. I. Chromatic responses and spectral saturation," J. Opt. Soc. Am. **45**, 546–552 (1955), digitized from Ref. 26. Cone fundamentals from Ref. 27. Equations (4)–(6) were integrated using an adaptive fourth-order Runge–Kutta routine (Scientist, MicroMath Research, Salt Lake City, UT) and fitted to the average of Jameson and Hurvich's data. The fit was done in ascending steps of 10 nm, with an adaptive integration step size between increments. Parameters a, d, and h were determined by linear stability analysis; the remaining six parameters were fit by least squares (see Table 1). No physiological significance should be vested in their values; they are not a unique solution, nor are they likely to be a global minimum, and are strictly of illustrative value.
26. J. Larimer, D. H. Krantz, and C. M. Cicerone, "Opponent process additivity. I. Red/green equilibria," Vision Res. **14**, 1127–1140 (1974).
27. A. Stockman, D. I. A. MacLeod, and N. E. Johnson, "Spectral sensitivities of the human cones," J. Opt. Soc. Am. A **10**, 2491–2521 (1993).
28. For example Eq. 4 could be modified to

$$\partial\omega_R/\partial_t = \omega_R[\mathrm{LC}^*(\lambda) - (a\,\omega_R + b\,\omega_G + c\,\omega_v)] + D_R(\partial^2\omega_R/\partial x^2 + \partial^2\omega_R/\partial y^2),$$

a Lotka–Volterra (LV) version of a reaction–diffusion (RD) equation. We take diffusion to be the prototypical filling-in mechanism (see Refs. 29 and 30). Both RD and diffusive LV systems are capable of spatiotemporal pattern formation (morphogenesis) for some parameterizations (in general, ω_R, ω_G, ω_V would need different diffusion rates or asymmetrical coupling, or cross diffusion). Such models give rise to transient or stable stationary spatial structures. A. Okubo, *Diffusion and Ecological Problems: Mathematical Models* (Springer, Berlin, 1980).

29. A. A. Baloch and S. Grossberg, "A neural model of high level motion processing," Vision Res. **37**, 3037–3059 (1997).
30. A good physical analogy is two separated reservoirs respectively filled with infinite supplies of red and green ink (at fixed concentrations). If connected by a long clear pipe, Eqs. (9) and (10) give the concentrations of red and green ink along the length of the pipe (at steady state). At steady state, the values of the diffusion rate constants are irrelevant. For a brief discussion of related issues see J. M. Smith, *Mathematical Ideas in Biology* (Cambridge U. Press, Cambridge, UK, 1971).
31. R. T. Eskew, Jr., "The gap effect revisited: Slow changes in chromatic sensitivity as affected by luminance and chromatic borders," Vision Res. **29**, 717–729 (1989).
32. For a review of related models of drug- and migraine-induced geometric hallucinations see O. W. Sacks and R. M. Siegal, "Migraine aura and hallucinatory constants," in *Migraine*, O. W. Sacks, ed. (Picador, London, 1992), pp. 273–297.
33. We can however speculate. Niebur *et al.*'s model of competition interactions uses frequency-gated inhibition; e.g., there is no inhibition unless the neural activity into the inhibitory mechanism falls within a particular spike rate (centered around gamma-band spike rates in the Niebur *et al.* model). E. Niebur, C. Koch, and C. Rosin, "An oscillation-based model for the neuronal basis of attention," Vision Res. **33**, 2789–2802 (1993). It is an interesting coincidence that during image stabilization, when stabilized images fade or fragment, the power ratio of alpha rhythm to higher-frequency components in the electroencephalogram (EEG) drastically increases just before and during image fading or fragmentation and wanes when images reappear (see Refs. 34 and 35). Why this happens is unclear, but if stabilization somehow eliminates higher-frequency neural activity, then it should also be expected to eliminate frequency-gated cortical competition. Such an analysis depends on drawing a tighter relationship between EEG spectra and the neural activity in specific cortical units [like those modeled in Eq. (4)–(6)] than we currently can.
34. D. Lehmann, G. W. Beeler, and D. H. Fender, "Changes in patterns of the human electroencephalogram during fluctuations of perception of stabilized retinal images," Electroencephalogr. Clin. Neurophysiol. **19**, 336–343 (1965).
35. U. T. Keesey and D. J. Nichols, "Fluctuations in target visibility as related to the alpha component of the electroencephalogram," Vision Res. **7**, 859–879 (1967).
36. T. Poggio, E. B. Gamble, and L. T. Little, "Parallel integration of visual modules," Science **242**, 436–440 (1988).
37. M. Barinaga, "Listening in on the brain," Science **280**, 376–378 (1998).